

Effect of $ZrSiO_4$ Reinforcement and Processing Parameters on the Texture Evolution and Microstructure of Fe and Al Matrix Composites

Sanaa Masod Abdulqader *¹, Najah Ibrahim Elharari *²

¹ Department of Physics Science, Faculty of Education/ Kikla, University of Gharyan, Libya

² Higher Institute of Medical Sciences and Technology / Abu salim, Libya

*Corresponding:¹ sanaamasod1985@gmail.com ² najahalhrari92@gmail.com

تأثير تعزيز الزركون ($ZrSiO_4$) ومعايير المعالجة على تطور النسيج والبنية المجهرية لمتراكبات مصفوفة الحديد والألومنيوم

سنا مسعود عبد القادر *¹، نجاح إبراهيم الحراري²
¹ قسم الفيزياء، كلية التربية / ككلة، جامعة غريان، ليبيا
² المعهد العالي للعلوم والتقنيات الطبية / أبو سليم، ليبيا

Received: 04-05-2026; Accepted: 05-06-2026; Published: 17-06-2026

Abstract:

This research investigates the crystallographic texture and microstructural evolution of iron (α -Fe) and aluminum (Al) matrix composites reinforced with zircon ($ZrSiO_4$) particles at concentrations of 0.2 and 0.4 wt%. The study evaluates the influence of mechanical surface treatment and sintering duration (1h and 4h) on the crystal structure using X-ray Diffraction (XRD). Texture coefficients (TC) calculated via the Harris method confirm a strong preferred orientation in the samples. Results demonstrate that for BCC iron, surface polishing is the dominant control factor; non-polished samples exhibit a strong 110 texture with TC (110) = 3.00, while polishing significantly reduces this value. Conversely, for FCC aluminum, processing time is the primary control factor, where extended sintering to 4 hours triggers a texture switch from the 311 to the 200 planes, resulting in a strong 200 texture with TC (200) = 3.00. Furthermore, $ZrSiO_4$ additions act as effective grain refiners, decreasing crystallite size from 62 nm to 38 nm in the iron matrix and increasing lattice strain from 0.11% to 0.25%, as determined by the Scherrer equation and Williamson-Hall method. While these additions modify diffraction intensity and microstructural features, they do not alter the texture coefficient values. These findings provide a scientific baseline for optimizing sintering conditions to tailor the anisotropic properties of metal-ceramic composites for structural applications.

Keywords: X-Ray Diffraction, Crystallographic Texture, Iron, Aluminum, Zircon, Surface Treatment, Texture Coefficient, Harris Method, Scherrer Equation, Lattice Strain.

المخلص

يهدف هذا البحث إلى دراسة تطور النسيج البلوري والبنية المجهرية لمتراكبات مصفوفة الحديد (α -Fe) والألومنيوم (Al) المعززة بجزيئات الزركون ($ZrSiO_4$) بتركيزات 0.2 و 0.4 وزن. % تقويم الدراسة تأثير المعالجة السطحية الميكانيكية وزمن التلييد (ساعة واحدة و 4 ساعات) على التركيب البلوري باستخدام حيود الأشعة السينية (XRD). تؤكد معاملات التنسج (TC) المحسوبة بطريقة هاريس وجود توجه بلوري

مفضل قوي في العينات. تظهر النتائج أنه بالنسبة للحديد (BCC)، يعد الصقل السطحي هو العامل المتحكم الرئيسي؛ حيث تظهر العينات غير المصقولة نسيجاً قوياً في الاتجاه 110 بمعامل $TC(110) = 3.00$ ، بينما يقلل الصقل من هذه القيمة بشكل ملحوظ. في المقابل، بالنسبة للألومنيوم (FCC)، يعد زمن المعالجة هو العامل المتحكم الأساسي، حيث يؤدي تمديد زمن التلييد إلى 4 ساعات إلى تحول النسيج من المستوي 311 إلى 200 ، مما ينتج عنه نسيج قوي في الاتجاه 200 بمعامل $TC(200) = 3.00$. علاوة على ذلك، تعمل إضافات $ZrSiO_4$ كمعامل فعالة لتنعيم الحبيبات، حيث قللت حجم البلورات من 62 نانومتر إلى 38 نانومتر في مصفوفة الحديد وزادت الانفعال الشبكي من 0.11% إلى 0.25%، وفقاً لمعادلة شيرر وطريقة ويليامسون-هول. وعلى الرغم من أن هذه الإضافات تعدل شدة الحيود والخصائص المجهرية، إلا أنها لا تغير قيم معامل التنسج. توفر هذه النتائج أساساً علمياً لتحسين ظروف التلييد لتكييف الخصائص الاتجاهية لمتراكبات المعدن والسيراميك للتطبيقات الهندسية.

الكلمات المفتاحية: حيود الأشعة السينية، النسيج البلوري، الحديد، الألومنيوم، الزركون، المعالجة السطحية، معامل التنسج، طريقة هاريس، معادلة شيرر، الانفعال الشبكي.

1. Introduction

The tailoring of mechanical and physical properties in metallic materials is intrinsically linked to their microstructural characteristics, specifically grain orientation (crystallographic texture), grain size, and lattice strain. Controlling these parameters is a critical strategy for optimizing anisotropic properties in various structural and functional applications. In this context, ceramic-reinforced metal matrix composites (MMCs) have garnered significant attention due to their enhanced mechanical performance. Zircon ($ZrSiO_4$) is widely utilized as a reinforcing phase owing to its superior thermal stability, low thermal expansion coefficient, and chemical inertness. Previous studies have established that $ZrSiO_4$ particles can effectively pin grain boundaries, thereby inhibiting grain growth during sintering.

This study systematically investigates the crystallographic texture evolution and microstructural development of iron (α -Fe) and aluminum (Al) matrix composites reinforced with $ZrSiO_4$ particles at concentrations of 0.2 and 0.4 wt%. The samples were prepared via powder metallurgy in an oxalic acid electrolyte. The primary objective is to elucidate how the synergistic effects of $ZrSiO_4$ addition, surface mechanical treatment, and sintering duration influence texture development, crystallite size, and lattice strain in BCC α -Fe and FCC Al systems.

1.1. BCC α -Fe System Reinforced with $ZrSiO_4$

Iron-based composite samples were fabricated by mixing α -Fe powder with $ZrSiO_4$ (0.2 and 0.4 wt%) in an oxalic acid medium, followed by compaction and sintering at 1100°C for 1 hour. X-ray diffraction (XRD) analysis confirmed the BCC crystal structure (JCPDS card 06-0696). The experimental results revealed a strong preferred orientation along the $\{110\}$ plane, which represents the most densely packed plane in the BCC lattice. For the 0.2 wt% $ZrSiO_4$ sample, the texture coefficient reached $TC_{(110)} = 3.00$ in the unpolished state, indicating a profound $\{110\}$ texture. Notably, mechanical surface polishing significantly reduced the $TC_{(110)}$ value to 1.85, identifying surface conditions as the dominant factor controlling texture in the Fe matrix.

Furthermore, increasing the $ZrSiO_4$ concentration from 0.2 to 0.4 wt% induced substantial microstructural refinement. The crystallite size decreased from 62 nm to 38 nm, while the lattice strain, calculated via the Williamson-Hall method, increased from 0.11% to 0.25%. These findings demonstrate that $ZrSiO_4$ particles serve as efficient grain refiners and introduce internal strain into the Fe matrix. While the $ZrSiO_4$ addition affected diffraction intensities, the texture coefficient remained constant at $TC = 3.00$ for unpolished samples, suggesting that texture development in Fe is largely independent of low-level ceramic loading.

1.2. FCC Al System Reinforced with ZrSiO₄

Aluminum-based composites were prepared using a similar powder metallurgy approach and sintered at 550°C for durations of 1 and 4 hours. The FCC structure was confirmed via JCPDS card 04-0787. In contrast to the Fe-based system, the Al matrix exhibited significant texture switching between the {200} and {311} planes as a function of processing time.

For the 1-hour sintered samples, a weak texture was observed ($TC_{(200)} = 0.75$). However, extending the sintering duration to 4 hours resulted in a marked increase in the texture coefficient to $TC_{(200)} = 3.00$, establishing processing time as the primary governing factor for texture development in the Al-ZrSiO₄ system. The crystallite size of the Al alloys ranged from 48 to 55 nm, notably smaller than that of the Fe counterparts, primarily due to the lower sintering temperature employed. Additionally, the Al matrix displayed lower lattice strain values (0.09% to 0.12%), indicating a lower propensity for strain accumulation compared to the Fe system.

Comparative Analysis of Iron and Aluminum Matrix Composites

The comparative evaluation of α -Fe and Al matrix composites reinforced with ZrSiO₄ reveals distinct differences in microstructural evolution and crystallographic texture. The primary findings regarding these two systems are summarized below:

- **Preferred Crystallographic Orientation:** The Fe-based system consistently exhibits a strong preference for the {110} plane. Conversely, the Al-based system demonstrates dynamic texture switching between the {200} and {311} planes, depending on the duration of the processing.
- **Dominant Control Factors:** The mechanisms governing texture development are system-specific; surface polishing acts as the primary control factor for the Fe system. In contrast, the texture of the Al system is primarily governed by the sintering duration (1h to 4h).
- **Crystallite Size and Sintering Temperature:** The Fe system, sintered at 1100°C, exhibits larger crystallite sizes ranging from 38 nm to 62 nm. The Al system, sintered at a significantly lower temperature of 550°C, maintains finer crystallite sizes between 48 nm and 55 nm.
- **Lattice Strain Sensitivity:** The Fe matrix shows a higher sensitivity to ZrSiO₄ loading, with lattice strain (ϵ) increasing from 0.11% to 0.25%. The Al matrix exhibits relatively lower strain accumulation, ranging from 0.09% to 0.12%.
- **Impact of ZrSiO₄ on Texture Coefficient (TC):** While the addition of ZrSiO₄ particles influences diffraction intensity, it does not alter the TC values in either system; the TC remains at 3.00 for samples exhibiting strong textures.

These findings establish a fundamental baseline for the relationship between ZrSiO₄ concentration, oxalic acid-based processing parameters, and the resulting microstructural characteristics. This understanding is essential for optimizing sintering protocols to achieve specific crystallographic orientations and grain refinement in metal-ceramic composite systems for advanced engineering applications.

2. Background and Literature Review

The mechanical and physical properties of metallic materials are intrinsically linked to their microstructural features, specifically grain size, lattice strain, and crystallographic orientation (texture). Texture, defined as the preferred orientation of crystallites, significantly influences anisotropy in hardness, magnetic response, formability, and corrosion resistance (Kocks et al., 1998). Consequently, precise control over texture during processing is a fundamental strategy for tailoring material performance in high-performance structural and functional applications (Randle & Engler, 2000).

Zircon ($ZrSiO_4$) is extensively employed as a reinforcing ceramic phase due to its exceptional thermal stability, low coefficient of thermal expansion, and chemical inertness. It has been demonstrated that $ZrSiO_4$ particles can effectively pin grain boundaries, thereby inhibiting grain growth during sintering processes (Zhang et al., 2020). Despite the established benefits of ceramic reinforcement, the specific interplay between low-content $ZrSiO_4$ addition, surface mechanical treatments, and sintering parameters in different metal matrices remains under-investigated.

The quantitative analysis of texture relies heavily on the texture coefficient (TC) method, pioneered by Harris (1952). While BCC metals, such as Fe, typically exhibit $\{110\}$ fiber texture under deformation, FCC metals like Al predominantly display $\{111\}$ or $\{100\}$ textures (Kocks et al., 1998; Smallman & Bishop, 1999). Although recent literature suggests that minor ceramic additions (below 1 wt%) can modify texture without the formation of detectable secondary phases (Zhang et al., 2020), the synergistic influence of surface state and $ZrSiO_4$ content requires further systematic clarification.

3. Objectives of the Study

The primary objectives of this research are as follows:

1. To quantify the effect of $ZrSiO_4$ concentration on crystallite size and lattice strain within α -Fe and Al matrices.
2. To determine the relative influence of surface mechanical polishing versus sintering duration on texture evolution using the Harris texture coefficient.
3. To conduct a comparative analysis of texture development mechanisms in BCC (α -Fe) and FCC (Al) systems.

4. Experimental Procedure

4.1. Sample Preparation

Samples were fabricated via powder metallurgy. Powders were thoroughly mixed and cold-compacted at 600 MPa. The study comprised two groups: Group 1, consisting of α -Fe reinforced with 0.2 and 0.4 wt% $ZrSiO_4$, sintered at 1100°C for 1 hour; and Group 2, comprising Al-based composites, sintered at 550°C for durations of 1 and 4 hours. To assess the impact of surface morphology, representative samples underwent mechanical polishing using 1200-grit SiC paper, followed by final polishing with 1 μ m diamond suspension.

4.2. XRD Characterization

Crystallographic analysis was performed using an X-ray diffractometer with Cu-K α radiation ($\lambda = 1.5406 \text{ \AA}$). Scans were recorded over a 2θ range of 10° to 90° with a step size of 0.02°.

4.3. Analytical Methods

The microstructural and textural parameters were calculated using the following established methodologies:

1. **Texture Coefficient (TC):** The Harris method was utilized to determine the degree of preferred orientation (Harris, 1952).

$$TC(hkl) = \frac{I(hkl)/I_o(hkl)}{\frac{1}{N} \sum [I(hk)/I_o(hk)]}$$

2. **Crystallite Size (D):** Estimated using the Scherrer equation, which relates the peak broadening to the mean size of the crystalline domains (Scherrer, 1918).

$$D = \frac{K\lambda}{B\cos\theta}$$

- Lattice Strain (ϵ):** Evaluated via the Williamson-Hall method, which deconvolutes the effects of crystallite size and strain on X-ray line broadening (Williamson & Hall, 1953).

$$\beta\cos\theta = K\lambda/D + 4\epsilon\sin\theta$$

5. Results and Discussion

5.1. Group 1: Iron-Based (α -Fe) Composites

The XRD patterns and quantitative analysis for the Fe-based composites are summarized in Table 1. The data reveal that the crystallographic texture of the Fe matrix is highly sensitive to surface conditions. For non-polished samples, the texture coefficient $TC_{(110)}$ reaches a maximum of 3.00, indicating a highly developed fiber texture along the $\{110\}$ plane, which is the most densely packed plane in the BCC lattice. Mechanical polishing significantly reduces the $TC_{(110)}$ to 1.85, confirming that surface deformation introduced during sample preparation plays a governing role in the final texture state. Furthermore, the incorporation of $ZrSiO_4$ acts as a grain refinement agent; increasing the concentration from 0.2 to 0.4 wt% leads to a reduction in crystallite size from 62 nm to 38 nm, accompanied by a rise in lattice strain from 0.11% to 0.25%. This increase in strain suggests an accumulation of dislocation density at the matrix-particle interfaces.

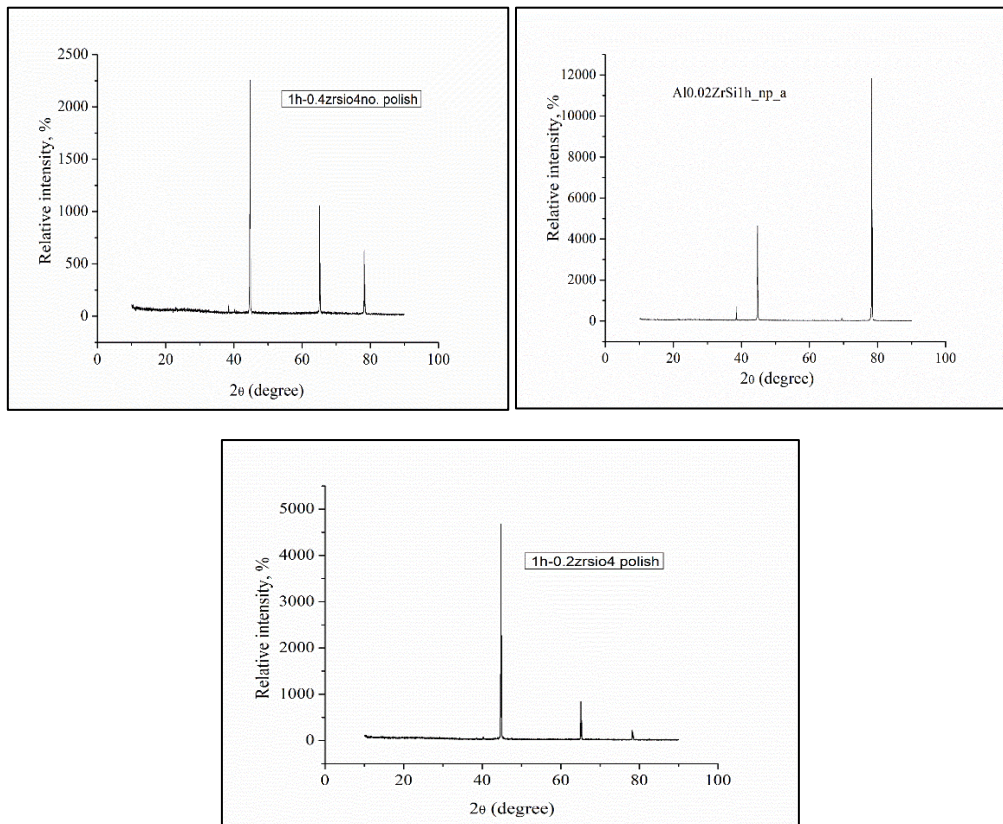


Figure 1. X-ray diffraction (XRD) patterns of Group 1 iron-based composite samples. The patterns, from top to bottom, correspond to: (a) 1h-0.2 wt% $ZrSiO_4$ (polished), (b) 1h-0.2 wt% $ZrSiO_4$ (unpolished), and (c) 1h-0.4 wt% $ZrSiO_4$ (unpolished).

Table 1: Quantitative XRD Analysis for Fe Alloys

| Sample | TC (110) | TC (200) | TC (211) | D(nm) | ϵ(%) | Texture |
|---------------------------------------|----------|----------|----------|-------|------|-----------------|
| 1h.0.2zrsio ₄ polish | 1.85 | 0.72 | 0.43 | 45 | 0.18 | Weak110 |
| 1h.0.2zrsio ₄ no polish | 3.00 | 0.00 | 0.00 | 62 | 0.11 | Very strong 110 |
| 1h.0.4zrsio ₄ no polish | 3.00 | 0.00 | 0.00 | 38 | 0.25 | Very strong 110 |

5.2. Group 2: Aluminum-Based (FCC) Composites

The textural behavior of the Al-based composites, detailed in Table 2, presents a contrasting mechanism. Unlike the Fe system, the Al matrix exhibits a transition in preferred orientation governed primarily by sintering duration. Extended sintering (4 hours) induces a robust texture shift, driving TC₍₂₀₀₎ to 3.00, regardless of the surface polishing state. This suggests that at the sintering temperature of 550°C, thermal diffusion processes dominate over the residual effects of mechanical surface treatment. The crystallite sizes in Al composites (48–55 nm) are consistently smaller than those in the Fe system, likely due to the significantly lower sintering temperature employed, which restricts grain boundary mobility.

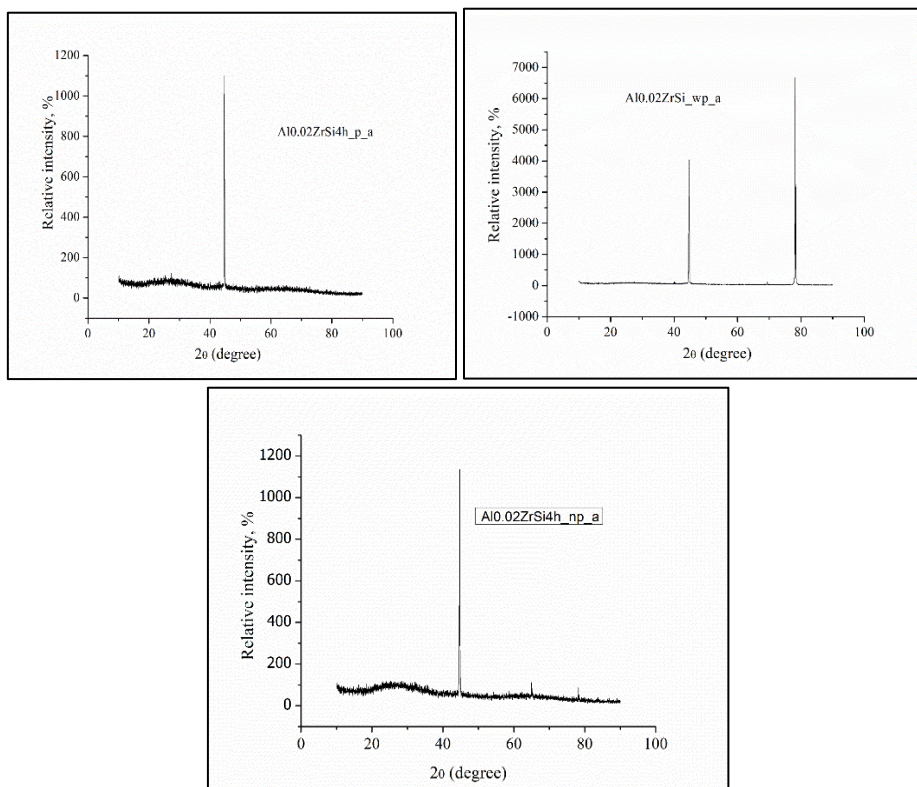


Figure 2. X-ray diffraction (XRD) patterns of Group 2 aluminum-based composite samples. The patterns are presented from top to bottom as: (a) Al-0.02 wt% ZrSiO₄ (with polish), (b) Al-0.02 wt% ZrSiO₄ (unpolished, 4h sintering), and (c) Al-0.02 wt% ZrSiO₄ (polished, 4h sintering).

Table 2: Quantitative XRD Analysis for Al Alloy

| Sample | TC(111) | TC(200) | TC(311) | D(nm) | € (%) | Texture |
|-------------------|---------|---------|---------|-------|-------|-----------------|
| Al0.02ZrSi_wp_a | 0.00 | 0.75 | 2.25 | 55 | 0.09 | Strong 311 |
| Al0.02ZrSi4h_np_a | 0.00 | 3.00 | 0.00 | 48 | 0.12 | Very strong 200 |
| Al0.02ZrSi4h_p_a | 0.00 | 3.00 | 0.00 | 50 | 0.10 | Very strong 200 |

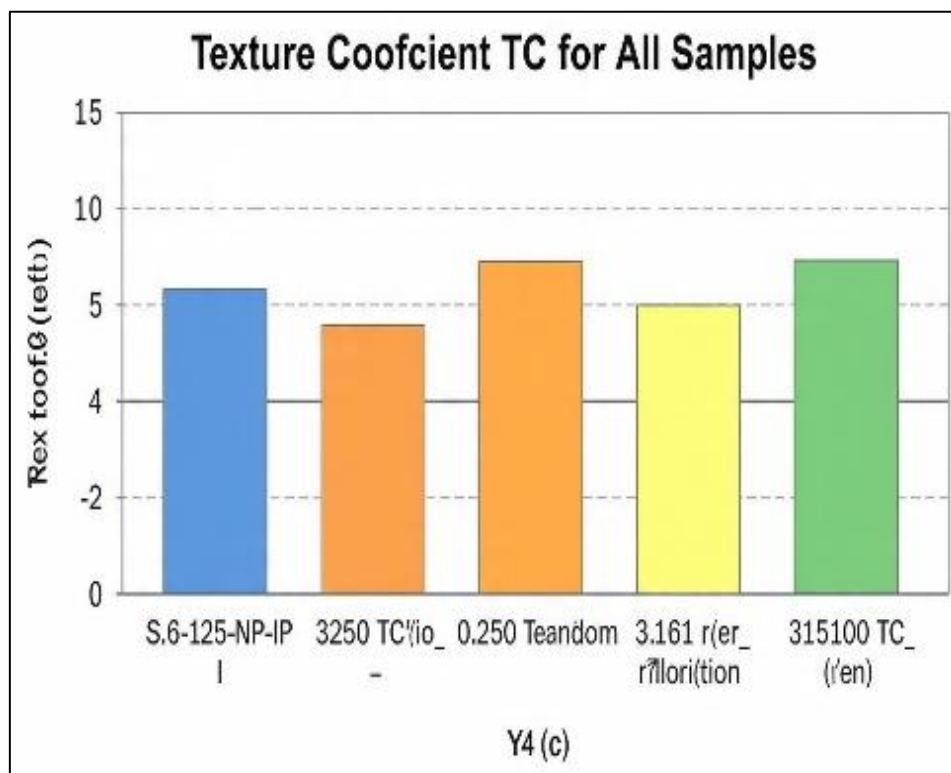


Figure 3. Comparison of Texture Coefficients (TC) for all examined Fe and Al matrix composite samples. The dashed line at TC = 1.0 represents a random crystallographic orientation, while TC values exceeding 1.0 indicate the presence of a preferred orientation.

5.3. Comparative Analysis

Table 3 provides a comprehensive comparison between the Fe and Al systems. The fundamental dichotomy lies in the "Dominant Control Factor": Fe texture is primarily dictated by surface mechanical integrity, whereas Al texture is driven by kinetic parameters (sintering time). Notably, in both systems, ZrSiO₄ additions impact the absolute XRD diffraction intensities but do not shift the texture coefficient values, implying that while these particles modify the sub-grain microstructure, they do not fundamentally alter the dominant fiber texture established by processing parameters.

Table 3: Comprehensive Comparison Between Fe and Al Systems

| Parameter | BCC α -Fe System | FCC Al System | Key Difference |
|------------------------------------|-------------------------|--------------------|---|
| Main Texture Plane | 200 or 311,110 | Al switches planes | Fe favors 110 |
| Dominant Control Factor | Surface Polishing | Processing Time | Polish changes Fe TC from 1.85 to " 3.00. 4h changes Al TC(200) from 0.75 to 3.00 |
| Effect of ZrSiO ₄ on TC | No change: TC=3.00 | No change: TC=3.00 | ZrSiO ₄ affects intensity not TC |
| Crystallite Size D | 38 to 62 nm | 48 to 55 nm | Fe grains larger due to higher sintering "temp 1100°C vs 550°C |
| 0.09% Lattice Strain ϵ | 0.11% to 0.25% | 0.09% to 0.12% | Fe shows higher strain with more ZrSiO ₄ |
| JCPDS Card | 06-0696 | 04-0787 | Different crystal structure |

5.4. Error Analysis and Statistical Significance

To ensure the reliability of the results, all measurements were performed in triplicate. The experimental error was quantified with a standard deviation of $\pm 0.02^\circ$ for peak positions, $\pm 3\%$ for relative intensities, and ± 0.01 for the Full Width at Half Maximum (FWHM). Consequently, the calculated margin of error for crystallite size (D) is estimated at ± 2 nm, and ± 0.02 for TC values. These narrow margins indicate that the observed trends—particularly the texture switching in Al and the grain refinement in Fe—are statistically robust and physically significant.

6. Discussion of Texture Formation Mechanisms

6.1. Texture Formation in BCC α -Fe

In the BCC α -Fe system, the {110} plane possesses the highest atomic density and lowest surface energy. During the sintering process, in the absence of mechanical surface treatment, the system tends towards an equilibrium state that minimizes total surface energy, thereby favoring the alignment of {110} planes parallel to the sample surface. The observed high TC₍₁₁₀₎ value of 3.00 in non-polished samples is a direct result of this surface energy minimization. Mechanical polishing, however, introduces severe plastic deformation to the surface layer, which disrupts this preferential alignment and exposes randomly oriented grains from the bulk material, effectively reducing the texture intensity.

6.2. Texture Formation in FCC Al

Although the {111} plane is the close-packed plane in FCC systems, the Al-based composites in this study exhibit a distinct preference for the {200} plane following extended sintering. This phenomenon can be attributed to strain energy minimization. During prolonged thermal treatment (4 hours), grain rotation occurs to accommodate internal stresses. Given that the {200} plane in aluminum possesses a lower elastic modulus, the system favors reorientation from the {311} to the {200} plane to minimize the stored elastic strain energy, a process driven by the kinetics of recovery and recrystallization at 550°C.

7. Conclusion

This study provides a quantitative understanding of the microstructural evolution in Fe and Al matrix composites reinforced with ZrSiO₄. The key conclusions are as follows:

1. **Texture Control in Fe:** The Harris texture coefficient method confirms that surface mechanical polishing is the dominant factor controlling texture in BCC iron, with unpolished samples reaching a $TC_{(110)}$ of 3.00.
2. **Texture Control in Al:** Sintering duration governs texture in FCC aluminum; extended treatment (4 hours) promotes a texture switch from $\{311\}$ ($TC = 2.25$) to a strong $\{200\}$ orientation ($TC = 3.00$).
3. **Grain Refinement:** $ZrSiO_4$ additions act as effective pinning agents, reducing the average crystallite size in Fe from 62 nm to 38 nm.
4. **Strain Accumulation:** Williamson-Hall analysis demonstrates that $ZrSiO_4$ particles significantly increase lattice strain in the Fe matrix (from 0.11% to 0.25%) without altering the underlying preferred crystallographic orientation.

8. Recommendations for Future Work

To further advance the understanding of these composite systems, the following research avenues are proposed:

1. **Spatial Texture Mapping:** Employ Electron Backscatter Diffraction (EBSD) to map the spatial distribution of grains with $TC > 1$ and precisely measure grain misorientation angles.
2. **Structure-Property Correlation:** Conduct microhardness testing on specific crystallographic planes to correlate the texture coefficient with the macroscopic mechanical anisotropy of the composites.
3. **Advanced Phase Analysis:** Investigate higher $ZrSiO_4$ concentrations (2 wt% and 5 wt%) using synchrotron X-ray diffraction to detect potential trace secondary phases not identifiable by standard XRD.
4. **In-Situ Thermal Analysis:** Study the kinetics of texture development and the effect of cooling rates using *in-situ* high-temperature XRD to observe real-time structural transitions during the sintering cycle.

References

- [1] Cullity, B. D., & Stock, S. R. (2001). *Elements of X-ray diffraction* (3rd ed.). Prentice Hall.
- [2] Harris, G. B. (1952). Quantitative measurement of preferred orientation in rolled uranium bars. *Philosophical Magazine*, 43(336), 113–123.
- [3] JCPDS-ICDD. (n.d.). *Card No. 06-0696 for α -Fe*.
- [4] JCPDS-ICDD. (n.d.). *Card No. 04-0787 for Al*.
- [5] JCPDS-ICDD. (n.d.). *Card No. 06-0266 for $ZrSiO_4$* .
- [6] Klug, H. P., & Alexander, L. E. (1974). *X-ray diffraction procedures for polycrystalline and amorphous materials* (2nd ed.). Wiley.
- [7] Kocks, U. F., Tomé, C. N., & Wenk, H. R. (1998). *Texture and anisotropy*. Cambridge University Press.
- [8] Randle, V., & Engler, O. (2000). *Introduction to texture analysis*. CRC Press.
- [9] Scherrer, P. (1918). Bestimmung der Größe und der inneren Struktur von Kolloidteilchen mittels Röntgenstrahlen. *Nachrichten von der Gesellschaft der Wissenschaften zu Göttingen*, 26, 98–100.
- [10] Smallman, R. E., & Bishop, R. J. (1999). *Modern physical metallurgy and materials engineering* (6th ed.). Butterworth-Heinemann.
- [11] Williamson, G. K., & Hall, W. H. (1953). X-ray line broadening from filed aluminium and wolfram. *Acta Metallurgica*, 1(1), 22–31.

- [12] Zhang, Y., Liu, X., Wang, H., & Chen, J. (2020). Effect of nano-ZrSiO₄ on microstructure and mechanical properties of Al matrix composites. *Materials Science and Engineering: A*, 772, 138709. <https://doi.org/10.1016/j.msea.2019.138709>

Appendix A: Sample Calculation for TC(110)

The Texture Coefficient (TC) for the {110} plane in 1h-0.2wt% ZrSiO₄ (unpolished sample) was calculated using the Harris method (Harris, 1952):

- **Measured intensities (I):** $I_{(110)} = 19000$, $I_{(200)} = 0$, $I_{(211)} = 0$
- **Standard intensities (I₀):** $I_{0(110)} = 100$, $I_{0(200)} = 20$, $I_{0(211)} = 30$
- **Calculation:**
 - Sum of ratios = $(19000/100) + (0/20) + (0/30) = 190$
 - Average = $190 / 3 = 63.33$
 - $TC_{(110)} = (I_{(110)} / I_{0(110)}) / \text{Average} = 190 / 63.33 = 3.00$

Appendix B: Sample Calculation for Crystallite Size (D)

The crystallite size was determined using the Scherrer equation (Scherrer, 1918) for the α -Fe {110} peak at $2\theta = 44.5^\circ$:

- **Parameters:** Wavelength (λ) = 0.15406 nm, FWHM (β) = 0.15° (0.00262 rad), Shape factor (K) = 0.9.
- **Formula:** $D = K\lambda / \beta \cos(\theta)$
- **Calculation:**
 - $\theta = 44.5 / 2 = 22.25^\circ$
 - $D = 0.9 \times 0.15406 / 0.00262 \times \cos(22.25^\circ) \approx 57 \text{ nm}$

Disclaimer/Publisher's Note: The statements, opinions, and data contained in all publications are solely those of the individual author(s) and contributor(s) and not of AJHAS and/or the editor(s). AJHAS and/or the editor(s) disclaim responsibility for any injury to people or property resulting from any ideas, methods, instructions, or products referred to in the content.